



Published in final edited form as:

J Photochem Photobiol B. 2021 July ; 220: 112212. doi:10.1016/j.jphotobiol.2021.112212.

Red light stimulates vasodilation through extracellular vesicle trafficking

Dorothee Weihrauch², Agnes Keszler¹, Brian Lindemer¹, John Krolkowski², Nicole L. Lohr^{1,3,4,*}

¹Department of Medicine- Division of Cardiovascular Medicine

²Department of Anesthesiology

³Cardiovascular Center, Medical College of Wisconsin

⁴Clement J Zablocki VA Medical Center

Abstract

Red light (670 nm) promotes ex vivo dilation of blood vessels in a nitric oxide (NO) dependent, but eNOS independent manner by secreting a quasi-stable and transferable vasoactive substance with the characteristics of S-nitrosothiols (RSNO) from the endothelium. In the present work we establish that 670 nm light mediated vasodilation occurs in vivo and is physiologically stable. Light exposure depletes intracellular S-nitroso protein while concomitantly increasing extracellular RNSO, suggesting vesicular pathways are involved. Furthermore, we demonstrate this RSNO vasodilator is embedded in extracellular vesicles (EV). The action of red light on vesicular trafficking appears to increase expression of endosome associated membrane protein CD63 in bovine aortic endothelial cells, enhance endosome localization in the endothelium, and induce exit of RSNO containing EVs from murine facialis arteries. We suggest a mechanism by which the concerted actions of 670 nm light initiate formation of RSNO containing EVs which exit the endothelium and trigger relaxation of smooth muscle cells.

Keywords

red light; extracellular vesicles; exocytosis; photobiomodulation; nitric oxide; endothelium; S-nitrosothiol

*Corresponding author at: Department of Medicine, Division of Cardiovascular Medicine, Medical College of Wisconsin, 8701 Watertown Plank Road, Milwaukee, Wisconsin 53226, ntonn@mcw.edu.

Author statement

Dorothee Weihrauch: Conceptualization, Methodology, Investigation. **Agnes Keszler:** Conceptualization, Investigation, Writing-Reviewing and Editing, **Brian Lindemer:** Conceptualization, Investigation, Writing- Reviewing and Editing, **John Krolkowski:** Investigation. **Nicole Lohr:** Supervision, Conceptualization, Writing original draft, Funding acquisition.

Publisher's Disclaimer: This is a PDF file of an unedited manuscript that has been accepted for publication. As a service to our customers we are providing this early version of the manuscript. The manuscript will undergo copyediting, typesetting, and review of the resulting proof before it is published in its final form. Please note that during the production process errors may be discovered which could affect the content, and all legal disclaimers that apply to the journal pertain.

Declaration of interests

The authors declare that they have no known competing financial interests or personal relationships that could have appeared to influence the work reported in this paper.

Introduction

Red light therapies represent a targeted, non-invasive treatment for a plethora of diseases connected with inflammation and wound healing, yet also hold significant potential to improve serious neurological and cardiovascular conditions (1, 2). However, its therapeutic application for complex disease is restrained by the broad characterization of red light's actions and the incomplete understanding of its mechanisms. Original mechanisms suggested the mitochondrion to be the primary target of 670 nm light treatment with resulting modulation of downstream energetic pathways (3). One putative mechanism involves nitric oxide (NO) mediated regulation of the mitochondrial complex IV (cytochrome c oxidase) by competing with oxygen for the same binding site and altering electron flow (4). However, our previous work suggests that red light can promptly liberate NO from precursor molecules, such as nitrosyl hemoglobin and myoglobin (HbNO, and MbNO), S-nitrosothiols (RSNO), and dinitrosyl iron complexes (DNIC) without the intermediacy of mitochondria, to regulate vasodilation (5–8). We have confirmed the etiology of the 670 nm light's action is not related to temperature increases.

We have also established that 670 nm light exposure leads to dilation of pre-constricted murine facialis arteries in an eNOS independent but NO dependent manner. Interestingly, the dilation by 670 nm light induced the release of a quasi-stable vasoactive substance, most probably RSNO that could be transferred to and dilate a naïve vessel. This unusual finding led to a hypothesis that the vasoactive RSNO substance is enveloped in extracellular vesicles whose release may be stimulated by red light. Vesicles are lipid bilayer enclosed cytosol particles containing proteins and other cellular material formed within and exit cells by various stimuli (9–11). Indeed, we detected an increased number of vesicles and a higher concentration of S-nitroso proteins in the vessel bath after red light exposure compared to control. In a cellular model, we found that the red light stimulates exocytosis and depletes S-nitroso protein level. Here we suggest a mechanism by which 670 nm light triggers RSNO containing vesicle production in the endothelium followed by exocytosis.

Materials and Methods

Materials

Anti-S-nitrosocysteine antibody was purchased from Abcam (Cambridge, MA) and lysosomal associated membrane protein 3 (CD63) was purchased from Santa Cruz Biotechnologies (Santa Cruz, CA). The styryl dye N - (3- Trimethylammoniumpropyl) – 4 - (6 - (4- (Dimethylamino) phenyl) hexatrienyl) Pyridium Dibromide (FM5–95) was purchased from ThermoFisher (Waltham, MA). All other materials used were Sigma-Aldrich (St. Louis, MO) products. LED light sources with power supply were purchased from Quantum Devices Inc., Barneveld, WI and NIR Technologies, Waukesha, WI. Power output was determined with X97 Optometer (Gigahertz Optic Gbmh, Turkenfeld, Germany).

Laser Doppler Perfusion Imaging

C57BL/6 mice (25.2 ± 0.3 g, $n = 8$) were purchased from Jackson Laboratories. All experimental procedures and protocols used in this investigation were reviewed and

approved by the Animal Care and Use Committee of the Medical College of Wisconsin. Furthermore, all procedures and protocols conformed to the *Guiding Principles in the Care and Use of Animals* of the American Physiologic Society and were in accordance with the *Guide for the Care and Use of Laboratory Animals*. For laser Doppler measurement mice were anesthetized with 1.25% isoflurane-O₂. Rectal temperature was maintained at 37.0 ± 0.5°C. The hair on the hindlimb and thigh region of the posterior side of the mouse was removed. Hindlimb perfusion was assessed noninvasively in the plantar foot (index of the overall leg perfusion) before and immediately after red light treatment (670 nm) by scanning laser-Doppler (model LD12-IR; Moor Instruments, Wilmington, DE). The left thigh received no light and served as control for each animal, the right thigh was treated with 0, 25, 50, and 100 mW/cm² of 670 nm light for 15 minutes resulting in overall fluence of 0, 22.5, 45, and 90 J/cm² of energy. A fiberoptic cable, which narrowly directed the light beam to the thigh, was utilized for light delivery. The fluence range was determined by previous performed studies (5,12). The distance between the light source and the skin was 1 inch. Doppler perfusion of the plantar foot was assessed within anatomically defined regions of interest, consisting of the hind paw margins. The change in Doppler Intensity Units pre- and post-red-light treatment was first determined in each paw. The difference between the red light treated paw and the control paw was then determined.

Pressure myography to assess vasodilation

Segments of facialis arteries (160–260 µm ID) from C57Bl6/J mice were transferred to a water-jacketed perfusion chamber and cannulated with two glass micropipettes (tip diameter ≈30 µm) at their in-situ length. The arteries were bathed in the PSS-equilibrated solution maintained at pH 7.4 and 37 °C. The micropipettes were connected to a reservoir filled with physiological saline solution and the arteries were pressurized to 60 mmHg. The internal diameter of the arteries was measured with a video system composed of a stereomicroscope (Olympus CK 40), a charge-coupled device camera (Panasonic GP-MF 602), a video monitor (Panasonic WV-BM 1410), and a video measuring apparatus (Boeckeler VIA-100).

After a 1-hour equilibration period, the arteries were pre-constricted by ~50% of their resting diameter with a thromboxane A₂ analog, U-46619. To test the ability of U46619 to achieve stable blood vessel diameters through the end of a 30 min period, we measured diameters in a separate group up to 45 min after steady state. Diameters did not change during this test period. The blood vessels were placed in the dark and once steady-state contraction was obtained, they were treated with 10 mW/cm² of 670 nm light (NIR Technologies, Waukesha, WI) for 10 minutes. Control samples were treated in the same way as above but remained in the dark for 10 minutes instead of being treated with 670 nm light. For stability experiments, the bath was removed and kept at 37°C for 30 minutes. It was then placed on a second naïve vessel.

Exosome tracking

The bath was removed and centrifuged at 2,000 g for 10 minutes at 4°C. The supernatant was then spun again in an ultracentrifuge at 55,000 g for 1 hour at 4°C. The remaining pellet was resuspended in 500 µL of PBS. Exosomes were counted and sized by Nanoparticle Tracking Analysis (NanoSight NS300, Malvern Instruments Ltd. Malvern, UK).

Cell culture

Bovine Aortic Endothelial Cells (BAECs) (Cell Applications Inc., San Diego, California) were cultured under standard conditions using media containing RPMI (ThermoFisher; Waltham, MA), 20% FBS (ATCC; Manassas, VA), 2 mM L-Glutamine, and 0.5% Pen/Strep. All plates and slides were treated with 2% gelatin prior to seeding. All experiments were performed using passages P5–P9. Cells were plated on 100 mm TPP cell culture dishes (Midwest Scientific, Valley Park, MO) and 4 chamber cell culture slides (CELLTREAT Scientific Products, Pepperell, MA).

Immunofluorescence

Immunofluorescence was performed on BAECs and extracellular vesicles harvested from the vessel bath. We compared 670nm irradiation to a no light control. Cultured cells were irradiated in media at 670 nm, 6 J/cm². Resuspended extracellular vesicle pellets of vessel bath fluid were mounted to slides using Cytospin centrifugation. Cytospin was performed at 4°C, for 5 minutes at 5000 g. Slides and Cytospin were post-fixed in 4% PFA. Cells were permeabilized in 0.5% Triton X for 5 minutes at room temperature. Samples were incubated with the primary antibodies for SNO-cys (1:75 dilution), CD63 (1:50 dilution) and von Willebrand Factor (vWF, 1:50) at 37°C for 30 minutes. After a series of washes with phosphate buffered saline, samples were stained with the according Alexa 488 conjugated secondary antibodies (either anti mouse or rabbit IgG, 1:1000 dilution, SCBT, Santa Cruz, CA). DAPI (1:1000 dilution) was used for nuclear staining of cells. To visualize intra and extracellular vesicles FM5–95 (1:50 dilution) was applied for 5 minutes at room temperature. Slides were mounted with Shur/Mount medium (Triangle Biomedical Sciences, Durham, NC) and cover slipped. Omitting the secondary antibody served as the negative control. Images were captured and quantified with a fluorescent Nikon Eclipse Ti2 microscope using NIKON Element software. For analysis, the pixel intensity of each cell or extracellular vesicle cluster were determined after compensating for background fluorescence by thresholding on minimal fluorescence. The threshold was maintained the same for each antibody labeling throughout experimental repetitions to minimize variability.

Ozone-based chemiluminescence

Cellular RSNO was detected with NO analyzer (Sievers Model 280i) in a reducing medium prepared daily from KI and I₂ in glacial acetic acid and double distilled water. BAECs were lysed in 50 mM potassium phosphate/1 mM diethylenetriamine pentaacetic acid and 50 mM N-ethylmaleimide. Nitrite was removed from the samples with sulfanilamide (100 mM in 2 N HCl, 10% vol/vol). RSNO was quantified based on the detector response for known amounts of S-nitrosoglutathione.

Statistics

A Student's one-tailed t-test was used for statistics, and $p < 0.05$ was considered statistically significant, and all data are reported as mean \pm standard error (SE) unless otherwise indicated.

Results

670 nm light vasodilation occurs in vivo and is physiologically stable

Previously we observed 670 nm energy mediates a NO-dependent, but eNOS independent dilation of ex vivo murine facial arteries and cannot be attributed to heat from the applied red-light source (5–8). Although red light's actions have been described in vivo with respect to collateral growth and ischemic preconditioning (12, 8), in vivo vasodilation has not been tested. Here we found a significant increase in paw blood flow (Figure 1A) after 22.5 J of 670 nm treatment to the thigh ($180.1 \text{ VIU} \pm \text{SD } 38.7$) vs. control ($27.9 \text{ VIU} \pm \text{SD } 17.8$, $p < .005$). Also noted, the increases in blood flow were irrespective of total fluence, with saturation achieved at 22.5 J. These findings support the hypothesis that light energy can penetrate the skin to produce significant increases in blood flow.

We previously described light's mechanism of vasodilation to require an intact endothelium and results in the production of a vasodilator substance released into the vessel bath. The vasodilator exhibited characteristics of S-nitrosothiols as the vasodilation can be modulated by RSNO reducing agent ascorbate (8). Furthermore, the 670 nm light produces enough energy to cleave the S-N bond of RSNO liberating nitric oxide. Recognizing the cleavage of the S-N bond is relatively fast (7), we tested the overall stability of the vasodilator substance contained within the bath solution and its ability to stimulate further vasodilation. We exposed murine facial arteries to 670 nm light under previously published conditions and as expected light stimulated vasodilation (Figure 1B). After light exposure, the vessel bath was maintained at 37°C for 30 minutes before adding the treated bath solution to an unexposed vessel. The unexposed vessel significantly dilated in the treated bath solution, suggesting the vasodilator produced from red light treatment was viable for prolonged periods at physiological temperatures.

Bath solution from 670 nm light treated vessels contains stable quantities of extracellular vesicles

The observed stability of the vasodilator in the bath solution suggested the NO precursor was protected from degradation and led to consideration of extracellular vesicles as a potential mechanism. Initial characterization of particle concentration and size was performed on the bath solution obtained after red light treatment of vessels (13). Figure 2A shows that the particle concentration increased from 4×10^7 to 2×10^8 particle/ml after light exposure ($n=3$). The mean particle size was unchanged between the populations and measured 300 nm with a wide range distribution varying from 50 to 700 nm (Figure S1). These results suggested more abundant presence of extracellular vesicles within the bath after red light treatment. Therefore, initial characterization of these particles was performed using markers to identify its cellular origin. There was a significant increase after red light treatment vs control in fluorescence intensity of lipid membrane marker lipophilic styryl FM 5–95 (17.25 vs 1.5), and endothelial marker vWF (6.75 vs 1.25) as well as colocalization of both markers (2.75 vs 1), $p < 0.05$. (Figure 2B).

S-nitrosothiols are present in extracellular vesicles collected from bath solution of 670 nm light treated vessels

Since previous work identified increases in RSNO levels within the bath solution after 670 nm light treatment, it was important to identify whether RSNO was present in the vesicular fraction of the bath. Immunofluorescence imaging using an anti-S-nitrosocysteine antibody was performed on the vesicular fraction of the bath collected from irradiated and unexposed control vessels. An additional control group where the bath was treated with HgCl₂ prior to immunofluorescence was performed to deplete RSNO, thereby verifying the specificity of the anti-S-nitrosocysteine signal. In Figure 3A, immunofluorescent imaging of the control bath solution indicates a measurable background fluorescence which is unaltered by HgCl₂ treatment. However, there is a significant increase in S-nitrosocysteine fluorescence (RSNO) in the red light treated group (50.23 vs 45.72, p<0.05) which can be reduced with HgCl₂ (44.62, p<0.02), suggesting RSNO is present. Moreover, when merged with the membrane marker FM-595 (red), Figure 3A shows an overlapping pattern suggesting the RSNO is present within a membrane vesicle.

Since the prevailing hypothesis is red light irradiation releases RSNO from endothelial cells, the expectation would be a concomitant decrease in intracellular RSNO after red light treatment. To test whether red light depletes cellular RSNO levels, S-nitrosocysteine immunofluorescence was tested in cultured endothelial cells (BAEC). Quantification of extracellular RSNO after red light treatment in BAEC was performed and indicated a significant fraction was present. Figure 3B indicates lower RSNO levels (green fluorescence) remained inside the cells after red light exposure (93.48 vs 136.9, p<0.002). The decrease of S-nitroso protein quantity in 670 nm light treated cells may be partially due to RSNO decomposition besides exocytosis. Mercuric chloride was applied as specificity control for RSNO (decrease to 65.24, p<0.005). Figure 3C indicates a significant increase in RSNO was detected in the HBSS buffer after red light treatment (1.1±0.2 nM) when compared to the unexposed control (0.62±0.13 nM, p<0.05).

The late endosomal marker, CD63, is increased with red light exposure

Since extracellular vesicles are identified within the bath after red light exposure, it was necessary to examine the trafficking patterns of intracellular vesicles as a potential mechanism for these observations. We examined the late endosomal marker, CD63, and FM 5–95 dye which binds to lipid containing structures including vesicles. There was a significant increase in CD63 fluorescence in the extracellular vesicles in bath collected from 670 nm light treated vessels (55.98 vs 44.93, p<0.05) (Figure 4A–B). In a cellular model (Figure 4C–D), evaluation of the intracellular staining patterns indicated FM 5–95 staining in control cells exhibits a perinuclear pattern with granular staining in the cytosol, and loss of the cytosolic staining with red light treatment (Figure 4C). Under control conditions, the CD63 staining is punctate and homogenous throughout the cell. With 670nm light treatment, there is an increased intensity of CD63 fluorescence (57.04 vs 51.61, p<0.05) (Figure 4D) and a shift in the pattern toward perinuclear localization. The merged panels accentuate the loss of cytosolic FM 5–95 staining in the red light treated cells. These findings suggest that 670 nm light can alter intracellular vesicle traffic at an early timepoint and is consistent with observations that vesicles are present at early timepoints after 670 nm light exposure.

Discussion

Previously we established endothelial RSNO regulates the red light's vasodilatory effect and depletion of RSNO by ascorbate attenuated the dilation (8). The present findings expand the current knowledge regarding red light mediated effects on the vasculature by suggesting intracellular RSNO is embedded in extracellular vesicles released by the endothelium. First, the vasodilator produced by R/NIR remains effective for at least 30 minutes after it is released from the endothelium and before it is added to a naïve vessel (Figure 1). This observed chemical stability extends our previous observations and led us to suggest it may be protected from degradation by encapsulation in an extracellular vesicle (6). Second, an elevated concentration of extracellular vesicles (mean diameter of 300 nm) can be detected in bath fluid of murine facial arteries subjected to red light induced dilation than before irradiation (Figure 2). Third, more S-nitroso protein can be measured in such bath compared to ambient light control (Figure 3A), with a compensatory reduction in the intracellular S-nitroso protein content (Figure 3B). Finally, markers for endothelial derived vesicles (vWF, CD63) are increased in the bath after red light treatment and co-localize with the sterol marker FM 5-95 (Figure 4).

Photoactivated vasodilation with NO participation holds a long history, however, the early observations were reduced to the action of polychromatic light or typically focused to the UV region (14, 15). Lately, the UV light-controlled modulation of NO stores in the skin has been studied and found to be RSNO-dependent (16–18). However, clinical applicability of NO generation by UV wavelengths is limited by the potentially deleterious effects of DNA mutagenesis (18,19). Therefore, the beneficial effects of longer wavelengths have gained appreciation (20) and been investigated (1). Although both short and long wavelengths induce NO dependent but eNOS independent vasorelaxation (21, 6, 8), the mechanisms driving the process are quite different. While electromagnetic energy in the UV range directly cleaves nitrite to NO, the photon energy of red light is insufficient for such photochemistry thus the mechanism is more complex including the photolysis of iron-nitrosyl heme proteins, S-nitrosothiols, and dinitrosyl iron complexes. The degree of complexity is further elevated by the transferrable nature of light induced vasodilation. More interesting is the perceived stability of the 670 nm light mediated bath to induce vasodilation in a light naïve vessel after a 30 min incubation at physiological temperature. To date there is limited evidence supporting red light mediated exocytosis of vasodilators. Blue and green light is reported to induce exocytosis of dividing cells by directly stimulating Opsin 3/4, but this pathway targets cGMP without NO or redox mediation, and Opsin does not possess vasoreactivity in a 620–750 nm spectral range (22–24). This is the first account of 670 nm light facilitating exocytosis, thus acting in a dualistic way by releasing NO from RSNO (7) and facilitating RSNO discharge from the endothelium prolonging the vasodilatory propensity (6, 8). Our results are aligned with previous hypotheses related to the concept of RSNO and NO mediated stores within the endothelium. It was Ignarro (25) who hypothesized the acidic environment of the lysosome would stabilize RSNO. Moreover, it was shown that L-NAME treated animals exhibit use-dependent loss of vasodilation with repetitive stimulation by acetylcholine and bradykinin, which suggests the presence of preformed NO pools exist within the endothelium (26).

Our studies are an initial characterization of 670 nm light generated extracellular vesicles according to their origin and composition using cultured BAECs as a model. Here we propose that 670 nm light induces endothelial formation of RSNO containing vesicles followed by exocytosis. Extracellular vesicles are cell derived membranous compartments with complex and variable composition and can be internalized by cells or docked on the surface, thus being capable to trigger various signaling events. They are classified by size with overlaps between groups: exosomes (30–150 nm), nanovesicles (30–100 nm), microvesicles (100–1000 nm), and apoptotic bodies (500–3000 nm) (9, 14, 27). Particle analysis of the bath solution using Nanosight yielded a mean diameter of 300 nm, which would favor microvesicles, however there was a significant distribution of particles (50–700 nm) reflecting the heterogenous nature of the bath. In these initial studies, direct visualization of the particles revealed some clumping which may increase the observed mean diameters. Given the heterogeneity of the samples we sought to further specify the cellular origin of the vesicles by using endothelial markers and common trafficking pathways.

Endocytic vesicles form by involution of the plasma membrane and are directed into the cytosol. Their material after being recycled in the lysosome exits the cell (28). Early phases of endocytosis can be studied using FM dyes (29), therefore we used them to characterize early actions of red light on vesicle transport. 670 nm light treatment redistributed vesicle staining patterns away from the cytosol and favoring the perinuclear region of the cell. We cannot exclude this loss of cytosolic staining is due to exocytosis. One well characterized pathway for vesicular trafficking through the plasma membrane utilizes the tetraspanin protein, CD63 (30–32). Significant increases of late endosome and lysosome associated membrane protein CD63 expression was detected in irradiated cells and vessel treated bath when compared to controls (Figures 4B & D).

It is important to recognize and discuss the limitations of this study. The results are descriptive due to the limited sample collected from the microvessel bath. The collection of extracellular vesicles occurs from the abluminal side, which prevents direct identification of the vessel endothelium as the source. Previously we have shown the transference of the vasodilator requires the endothelium, as bath transfer experiments performed with denuded vessels do not elicit vasodilation (6). Finally, the issue of light generating heat as a confounder, however, we have previously demonstrated that the heat from the LED light source per se did not cause meaningful vasodilation (7).

In conclusion, we suggest an overall mechanism of the red light-initiated exocytosis of vasodilatory substances from the endothelium (Figure 5). Red light (670 nm) facilitates endocytosis and NO release from cytosolic RSNO (7). Vesicles containing abundant RSNO and NO exit the endothelium and elicit relaxation of smooth muscle cells with a concerted action of those two species supporting that RSNO mediated vasodilation may need RSNO independent NO as recently reported (33). Detailed examination of specific pathways, investigation of other key participants in endocytosis and exocytosis, and fine tuning the proposed mechanism are subject of current investigations.

Supplementary Material

Refer to Web version on PubMed Central for supplementary material.

Acknowledgement

The authors thank Grant Broeckel for editing support and Claudia Gohr and Elizabeth Mitton-Fitzgerald for assistance with the Nanoparticle Tracking Analysis.

Funding

This work was supported by the NHLBI HL139557(NL) and Veteran Health Administration I01BX004675 (NL), 1IK2BX002426 (NL).

Abbreviation

eNOS	endothelial nitric oxide synthase
EV	extracellular vesicle
HbNO	nitrosyl hemoglobin
MbNO	nitrosyl myoglobin
DNIC	dinitrosyl iron complexes
RSNO	S-nitrosothiols
PBS	phosphate buffer saline
HBSS	Hank's Balanced Salt Solution
BAECs	Bovine Aortic Endothelial Cells
oxyHb	oxyhemoglobin
SE	standard error

References

1. Chung H, Dai T, Sharma SK, Huang YY, Carroll JD, Hamblin MR: The nuts and bolts of low-level (light) therapy. *Ann. Biomed. Eng.* 40(2012)516–533 DOI: 10.1007/s10439-011-0454-7
2. Freitas L, Hamblin MR: Proposed mechanism of photobiomodulation or low-level light therapy. *IEEE J. Sel. Top Quantum Electron* 22(2016) DOI: 10.1109/JSTQE.2016.2561201
3. Karu T: primary and secondary mechanisms of action of visible and near-IR radiation on cells. *J. Photochem. Photobiol. B: Biol* 49(1999)1–17
4. Toledo JC, Augusto O: Connecting the chemical and biological properties of nitric oxide. *Chem. Res. Toxicol* 25(2012)975–989 [PubMed: 22449080]
5. Lohr NL, Kesler A, Pratt P, Bienengraber M, Wartier DC, Hogg N: Enhancement of nitric oxide release from nitrosyl hemoglobin and nitrosyl myoglobin by red/near infrared radiation: Potential role in cardioprotection. *J. Mol. Cell Cardiol* 47(2009)256–263 [PubMed: 19328206]
6. Kesler A, Lindemer B, Weichrauch D, Jones D, Hogg N, Lohr NL: Red/near infrared light stimulates release of an endothelium dependent vasodilator and rescues vascular function in a diabetes model. *Free Radic. Biol. Med* 113(2017)157–164 [PubMed: 28935419]

7. Keszler A, Lindemer B, Hogg N, Weihrauch D, Lohr NL: Wavelength-dependence of vasodilation and NO release from s-nitrosothiols and dinitrosyl iron complexes by far red/near infrared light. *Arch. Biochem. Biophys* 649(2018)47–52 [PubMed: 29752896]
8. Keszler A, Lindemer B, Hogg N, Lohr NL: Ascorbate attenuates red light mediated vasodilation: Potential role of S-nitrosothiols. *Redox Biology* 20(2019)13–18 [PubMed: 30261342]
9. French KC, Antonyak MA, Cerione RA: Extracellular vesicles docking at the cellular port: Extracellular vesicle binding and uptake. *Seminars Cell Develop. Biol* 67(2017)48–55
10. Atienzar-Aroca S, Flores-Bellver M, Serrano-Heras G, Martinez-Gil N, Barcia JM, Aparicio S, Perez-Cremades D, Garcia-Verdugo JM, Diaz-Llopis M, Romero FJ: Oxidative stress in retinal pigment epithelium cells increases exosome secretion and promotes angiogenesis in endothelial cells. *J. Cell. Mol. Med* 20(2016)1457–66 [PubMed: 26999719]
11. de Jong OG, Verhaar MC, Chen Y, Vader P, Gremmels H, Posthuma G, Schiffelers RM, Gucek M, van Balkom BW: Cellular stress conditions are reflected in the protein and RNA content of endothelial cell-derived exosomes. *J. Extracell. Ves* 1(2012)18396
12. Lohr NL, Ninomiya JT, Warltier DC, Weihrauch: Far red/near infrared light treatment promotes femoral artery collateralization in the ischemic hindlimb. *J. Mol. Cell. Cardiol* 62(2013)36–42 [PubMed: 23702287]
13. Dragovic RA, Gardiner C, Brooks AS, Tannetta DS, Ferguson DJP, Hole P, Carr B, Redman CWG, Harris AL, Dobson PJ, Harrison P, Sargent IL: Sizing and phenotyping of cellular vesicles using Nanoparticle Tracking analysis. *Nanomed. Nanotech. Biol Med* 7(2011)780–788
14. Furchgott RF, Ehreich SJ, Greenblatt E: The photoactivated relaxation of smooth muscle of rabbit aorta. *J. Gen. Physiol* 44(1961)499–519 [PubMed: 13702637]
15. Matsunaga F, Furchgott RF: Interaction of light and sodium nitrite producing relaxation of rabbit aorta. *J. Pharm. Exp. Ther* 248(1989)687–695
16. Monaghan C, McIlvenna LC, Liddle L, Burleigh M, Weller RB, Fernandez BO, Feelisch M, Muggerridge DJ, Easton C: The effect of two different doses of ultraviolet-A light exposure on nitric oxide metabolites and cardiorespiratory outcomes. *Eur. J. Appl. Physiol* 111(118)1043–1052
17. Pelegrino MT, Paganotti A, Seabra AB, Weller RB: Photochemistry of nitric oxide and S-nitrosothiols in human skin. *Histochem. Cell Biol* 153(2020)431–441 [PubMed: 32162135]
18. Pelegrino MT, Weller RB, Paganotti A, Seabra AB: Delivering nitric oxide into human skin from encapsulated S-nitrosoglutathione under UV light: An in vitro and ex vivo study. *Nitric Oxide* 94(2020)108–113 [PubMed: 31759127]
19. Khan AQ, Travers JB, Kemp MG: Roles of UVA radiation and DNA damage responses in melanoma pathogenesis. *Environ Mol Mutagen.* 59(2018):438–460. [PubMed: 29466611]
20. Kana JS, Hutschenreiter G, Haina D, Waidelich W: Effect of low-power density laser radiation on healing of open skin wounds in rats. *Arch. Surg* 116(1981)293–296 [PubMed: 7469766]
21. Andrews KL, McGuire JJ, Triggle CR: A photosensitive vascular smooth muscle store of nitric oxide in mouse aorta: no dependence on expression of endothelial nitric oxide synthase. *B. J. Pharm* 138(2003)932–940
22. Henkel AW, Upmann I, Bartl CR, Bonsch D, Reichard C, Maler JM, Nurnberger M, Umstatter R, Reulbach U, Kornhuber J, Wiltfang J: Light-induced exocytosis in development and differentiation. *J. Cell. Biochem* 97(2006)1393–1406 [PubMed: 16365884]
23. Ortiz SB, Hori D, Nomura Y, Yun X, Jiang H, Yong H, Chen J, Paek S, Pabdey D, Sikka G, Bhatta A, Gillard A, Steppan J, Kim JH, Adachi H, Barodka VM, Romer L, An SS, Shimoda LA, Santhanam L, Berkowitz DE: Opsin 3 nad 4 mediate light-induced pulmonary vasorelaxation that is potentiated by G protein-coupled receptor kinase 2 inhibitor. *Am. J. Physiol. Lung Cell Mol. Physiol* 314(2018) L93–L106 [PubMed: 28882814]
24. Sikka G, Hussmann GP, Pandey D, Cao S, Hori D, Park JT, Steppan J, Kim JH, Barodka V, Myers AC, Santhanam L, Nyhan D, Halushka MK, Koeler RC, Snyder SH, Shimoda LA, Berkowitz DE: Melanopsin mediates light-dependent relaxation in blood vessels. *Proc. Nat. Am. Soc* 111(2016)17977–17982
25. Ignarro LJ: Nitric Oxide. A novel signal transduction mechanism for transcellular communication. *Hypertension* 16(1990)477–483 [PubMed: 1977698]

26. Davisson RL, Bates JN, Johnson AK, Lewis SJ: Use-dependent loss of acetylcholine- and bradykinin-mediated vasodilation after nitric oxide synthase inhibition. Evidence for preformed stores of nitric oxide-containing factors in vascular endothelial cells. *Hypertension* 28(1996)354–360 [PubMed: 8794816]
27. Welsh J, Holloway JA, Wilkinson JS, Englyst NA: Extracellular vesicle flow cytometry analysis and standardization. *Frontiers Cell Develop. Biol* 2017 DOI: 10.3389/fcell.2017.00078
28. Settembre C, Fraldi A, Medina DL, Ballabio A: Signals from the lysosome: a control center for cellular clearance and energy metabolism. *Nat. Rev. Mol. Cell. Biol* 14(2013)283–296 [PubMed: 23609508]
29. Hines JH, Henle SJ, Carlstrom LP, Abu-Rub M, Henley JR: Single vesicle imaging indicates distinct modes of rapid membrane retrieval during nerve growth. *BMC Biology* 10(2014)4
30. Kobayashi T, Vischer UM, Rosnoblet C, Lebrand C, Lindsay M, Parton RG, Kruithof EKO, Gruenberg J: The tetraspanin CD63/lamp3 cycles between endocytic and secretory compartments in human endothelial cells. *Mol. Biol. Cell* 11(2000)1829–1843 [PubMed: 10793155]
31. Pols MS, Klumperman J: Trafficking and function of the tetraspanin CD63. *Exp. Cell Res* 315(2009)1584–1592. [PubMed: 18930046]
32. Hromada C, Muhleder S, Grillari J, Redl H, Holnthoner W: Endothelial extracellular vesicles – Promises and challenges. *Frontiers Physiol.* 2017 DOI: 10.3389/fphys.2017.00275
33. Liu T, Zhang M, Terry MH, Schroeder H, Wilson SM, Power GG, Li Q, Tipple TE, Borchardt D, Blood AB: Nitrite potentiates the vasodilatory signaling of S-nitrosothiol. *Nitric Oxide* 75(2018)60–69 [PubMed: 29428841]

Highlights

- Red light (670 nm) generates a stable vasodilator from arteries.
- Endothelial derived extracellular vesicles increase after light treatment.
- S-Nitrosothiols increase within endothelial derived vesicles after light treatment.

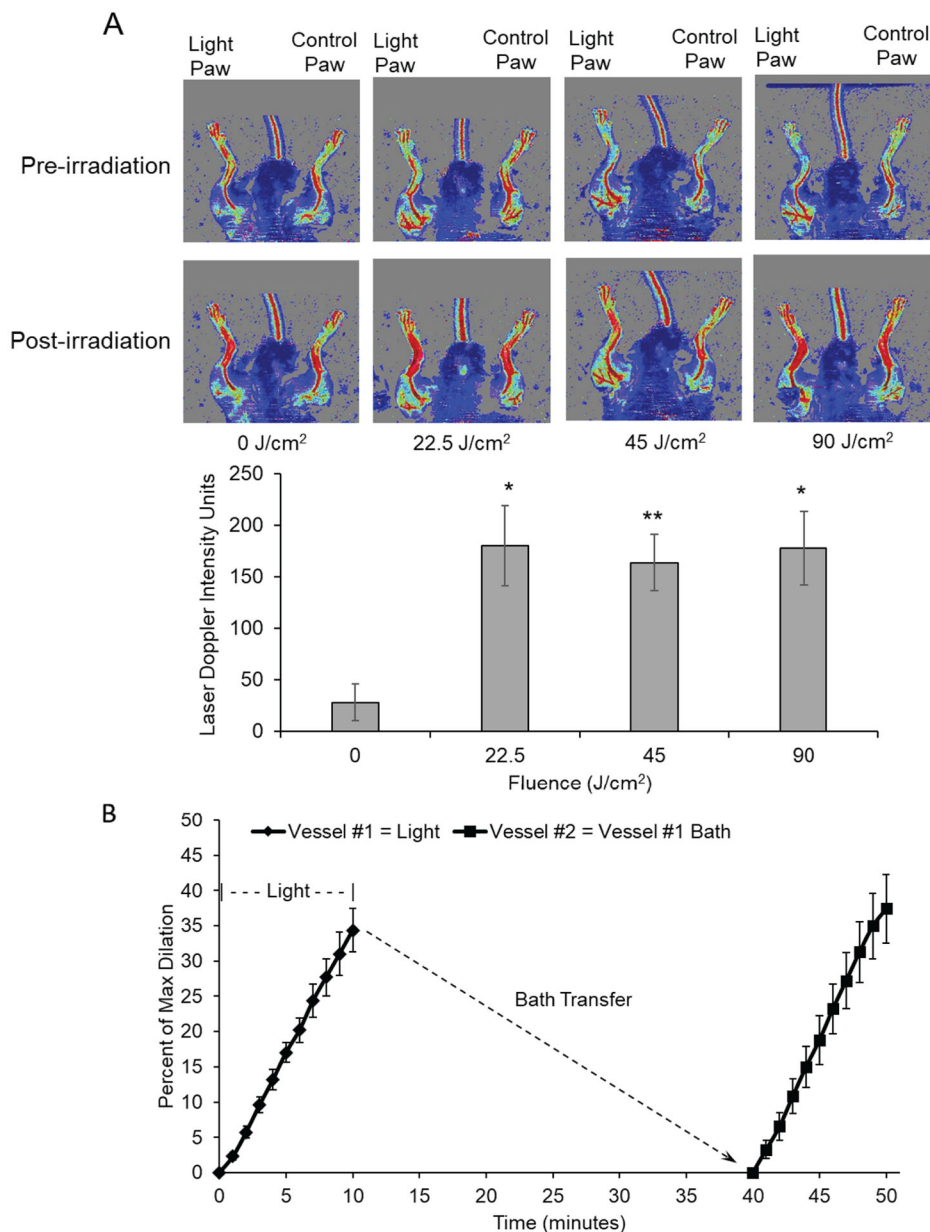


Figure 1. Vasodilatory effect of red light.

A: Laser doppler measurement of blood flow in hind limb of C57Bl/6 mice. 670 nm light was applied at increasing intensities (25, 50, 100 mW/cm²) for 15 min. The flow was measured as a difference between the irradiated limb and the other (control) limb of each animal. Upper: Representative image. Lower: Quantification. Values are mean±SE, *p<0.005, **p<0.001 vs. Control B: Red light induces exertion of stable vasodilatory agent from pre-constricted murine facialis arteries. Red light (670 nm, 6 J/cm²) induced dilation of primary blood vessel as measured by pressure myography. The bath buffer was collected, and after 30 min transferred to dilate a second naïve vessel..

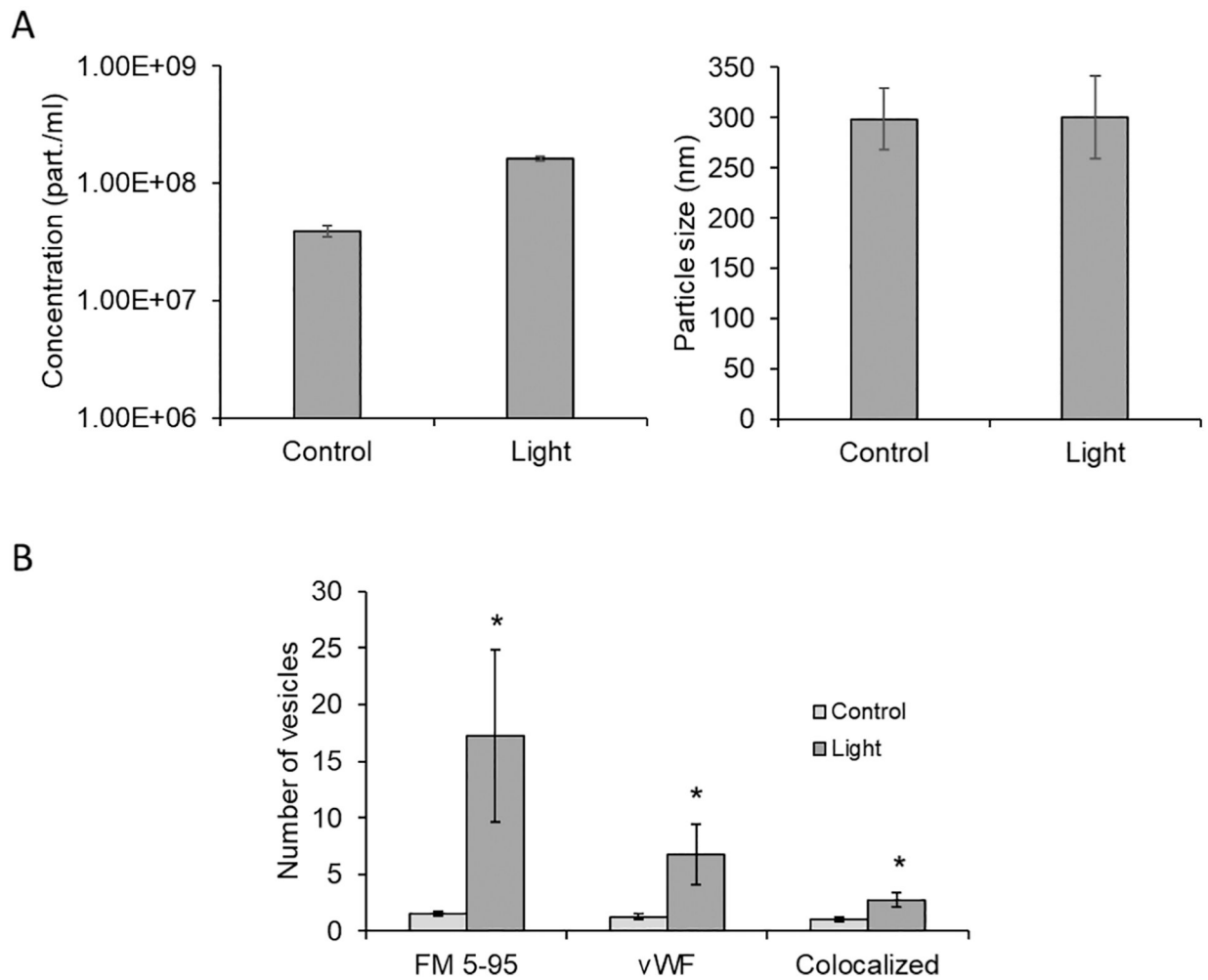


Figure 2. Red light induced exocytosis from pre-constricted murine facialis arteries. Red light (670 nm, 6 J/cm²) induced dilation of blood vessel measured by pressure myography. The bath buffer was collected, centrifuged, and pelleted. (A): Extracellular vesicles in the reconstructed pellet were characterized using NanoSight particle tracking analyzer. (B): Endothelial origin was characterized by vesicle marker FM 5–95 and its colocalization with endothelial marker vWF. Values are mean±SE, *p<0.05 vs. Control.

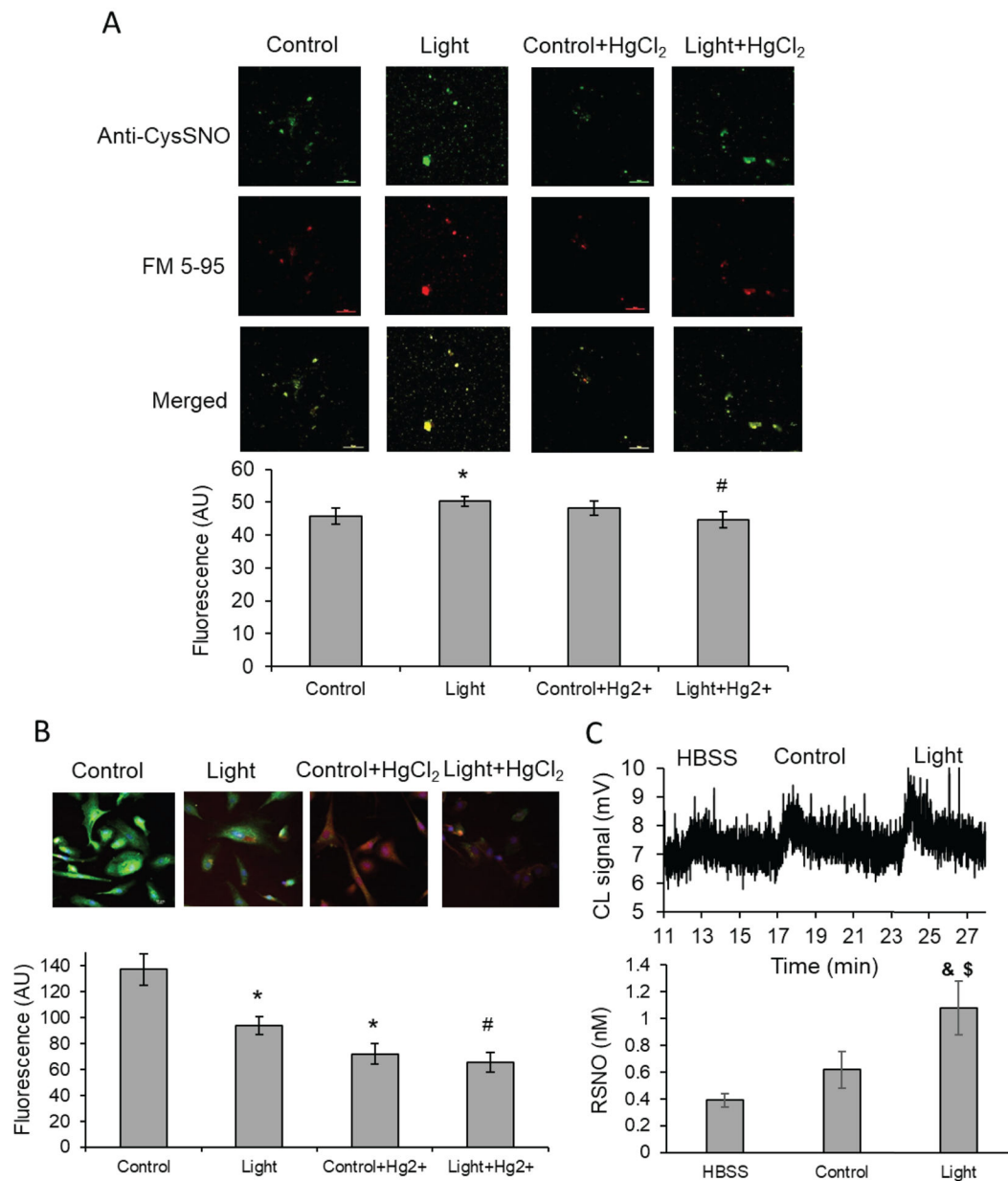


Figure 3. Red light mediated S-nitrosoprotein release from blood vessels and from BAECs.

(A) Red light (670 nm, 6 J/cm²) induced dilation of blood vessel. The bath buffer was collected, centrifuged, pelleted. S-nitrosoprotein formation was detected with anti-S-nitrosocysteine antibody (green), and its co-localization with FM 5–95 membrane marker dye (red) was recognized. *p<0.05 vs. Control, #p<0.02 vs. Light. (B): BAECs were exposed to light (670 nm, 6 J/cm²) and S-nitrosoprotein formation was detected with anti-S-nitrosocysteine antibody (green). DAPI staining marks the nuclei (blue). *p<0.002 vs. Control, #p<0.005 vs. Light. Mercuric chloride was applied as specificity control for RSNO. (C): BAECs were irradiated in HBSS (670 nm, 6 J/cm²), and medium were collected. Up: Representative chemiluminescence trace. Down: Quantification with S-nitrosoglutathione

standard. RSNO level increase in light treated sample was significant compared to HBSS control ($p < 0.02$) and ambient light control ($p < 0.05$). Values are mean \pm SE.

Author Manuscript

Author Manuscript

Author Manuscript

Author Manuscript

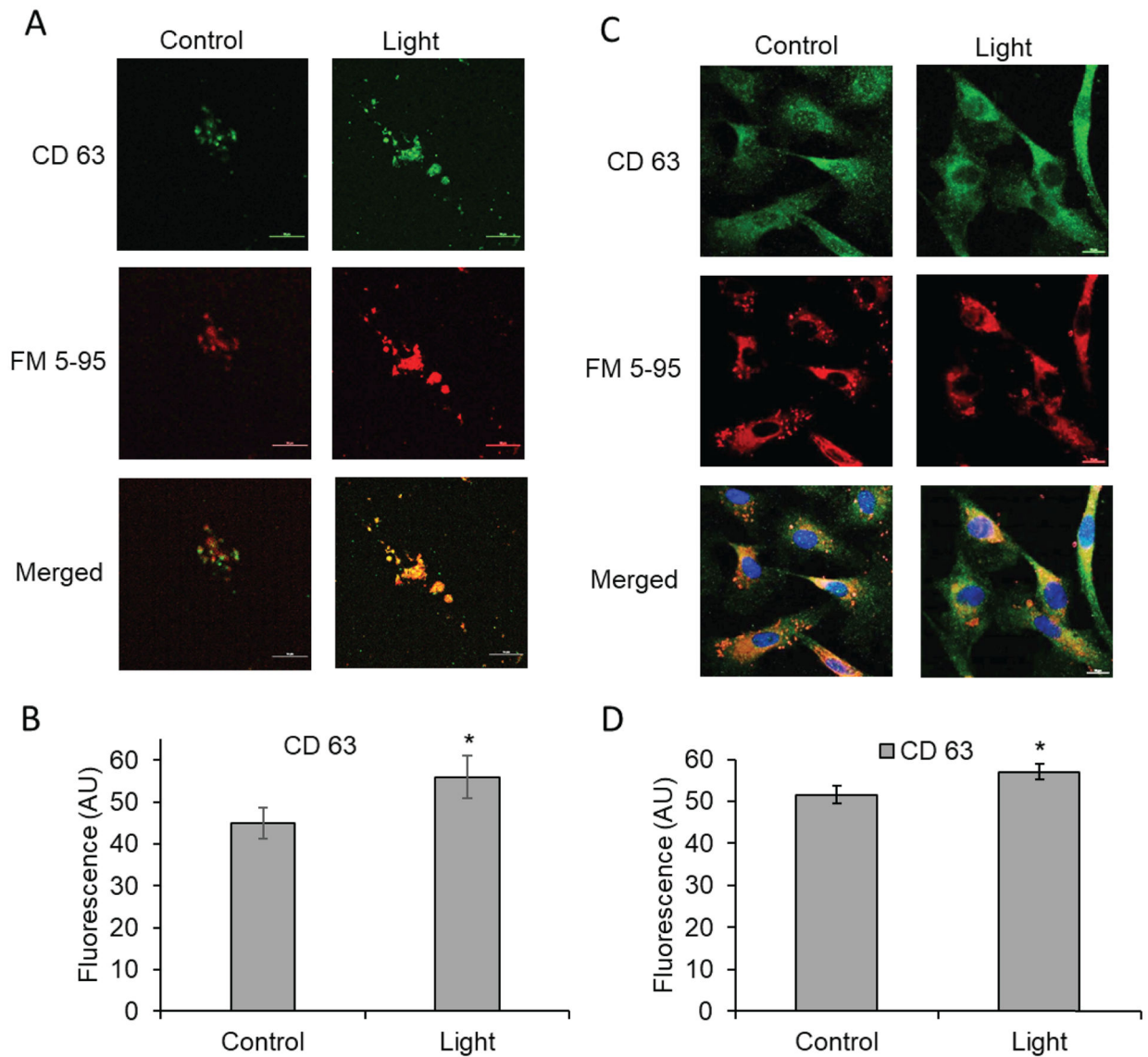


Figure 4. Red light effect on vesicle trafficking.

(A,B): Red light (670 nm, 6 J/cm²) induced dilation of blood vessel, and the bath buffer was collected, centrifuged, and pelleted. Increase of late endosomal marker CD 63 (green), and its co-localization with FM 5–95 membrane marker (red) were recognized. (C, D): BAECs were exposed to light (670 nm, 6 J/cm²). Vesicle formation was detected with immunofluorescence. Green: antibody of CD 63 endosome marker; red: FM 5–95; membrane marker dye. Blue: nucleus DAPI staining. Values are mean±SE, *p<0.05.

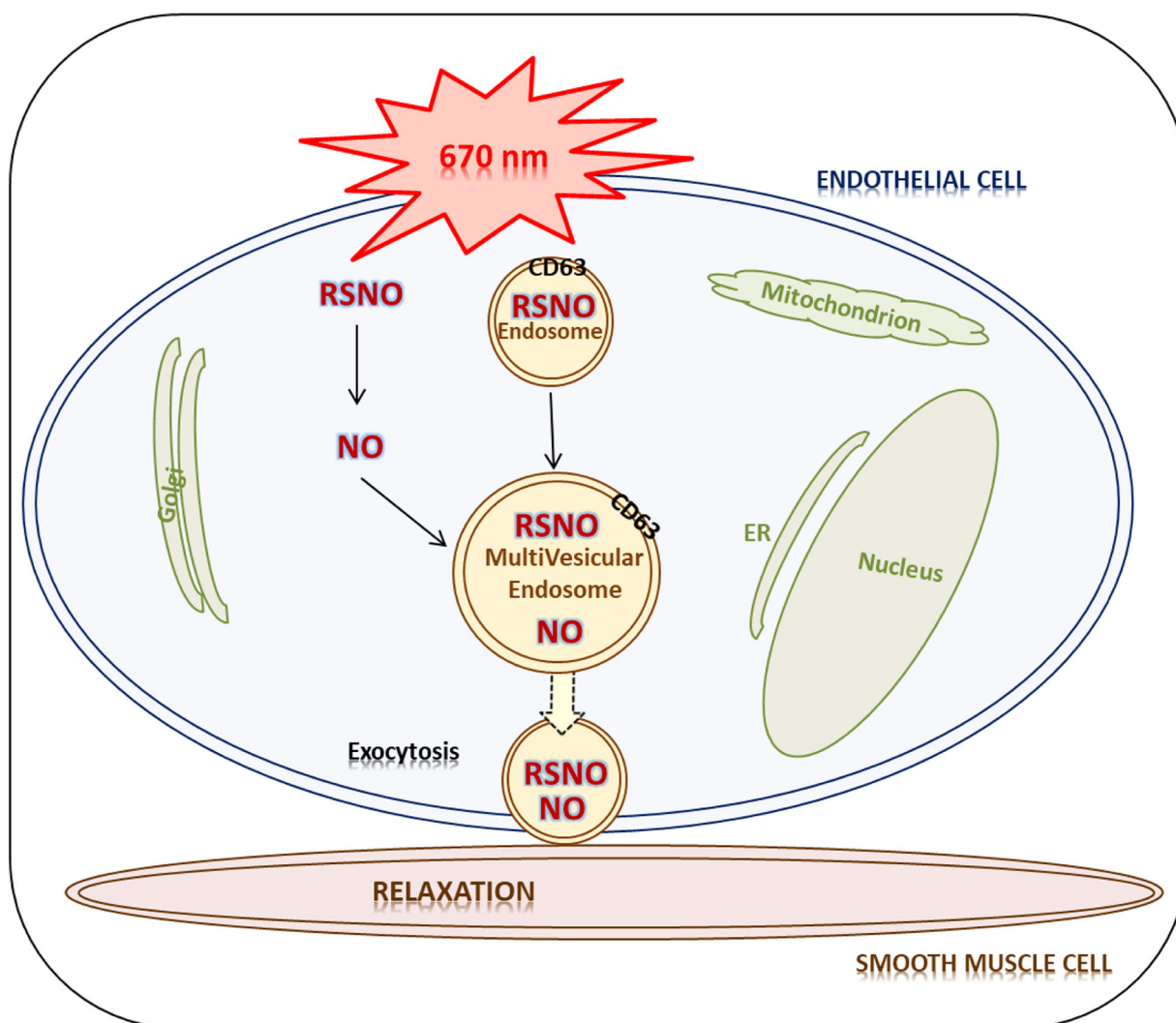


Figure 5. Mechanism of red light mediated exocytosis leading to vasodilation. Red light (670 nm) triggers endosome formation and subsequent exocytosis. The light also induces NO release from cytosolic RSNO. Protein RSNO and NO accumulate in vesicles which exit the endothelium and elicit dilation of smooth muscle cells.